

# We are IntechOpen, the world's leading publisher of Open Access books Built by scientists, for scientists

6,900

Open access books available

186,000

International authors and editors

200M

Downloads

Our authors are among the

154

Countries delivered to

TOP 1%

most cited scientists

12.2%

Contributors from top 500 universities



WEB OF SCIENCE™

Selection of our books indexed in the Book Citation Index  
in Web of Science™ Core Collection (BKCI)

Interested in publishing with us?  
Contact [book.department@intechopen.com](mailto:book.department@intechopen.com)

Numbers displayed above are based on latest data collected.  
For more information visit [www.intechopen.com](http://www.intechopen.com)



---

# The Impact of Ice Cover and Sediment Nonuniformity on Erosion Around Hydraulic Structures

---

Peng Wu, Jueyi Sui and Ram Balachandar

Additional information is available at the end of the chapter

<http://dx.doi.org/10.5772/61468>

---

## Abstract

Based on two case studies, the impact of ice cover on local scour around bridge piers is presented in this chapter. Bed material with different grain sizes is used and ice covers with different roughness is used to study the scour characteristics. The impact of nonuniformity of sediment is also investigated. Results show that with the increase in densimetric Froude number, there is a corresponding increase in the dimensionless scour depth. For nonuniform sediment, due to the formation of an armor layer, less maximum scour depth was noted around bridge foundation structures compared to uniformly distributed sediment. The increase in ice cover roughness results in a larger scour depth and geometry. The results indicate that it is imperative to pay attention to the impact of ice cover on the scour around hydraulic structures.

**Keywords:** ice cover, local scour, non-uniform sand, bridge abutment

---

## 1. Introduction

### 1.1. Sediment transport around hydraulic structures

Sediment transport embodies the processes of erosion, entrainment, movement, and deposition. In nature, these processes are always present. Although there are many types of sediment, fluvial sediment is one of the most common. It comprises sediment accumulated by the erosion of rock and mineral particles that are transported by flowing water. The process of erosion is complex and plays a vital role in the formation of different landscapes of the world we live in.

Statistics show that thirteen of the large rivers in the world carry sediment loads in excess of 5.8 billion tons annually [5]. In addition to producing large quantities of sediment, erosion also causes other problems such as the pollution of water body and altering the runoff conditions.

---

Additionally, from the perspective of hydraulic engineering, sediment transport can result in serious on-site damage to hydraulic structures such as bridge abutments, bridge piers, spur dikes, etc.

The presence of a hydraulic structure in a river introduces the phenomenon of local scour. The interaction between flow and structures has been an actively researched topic in the past decade. Reynolds stress is an important parameter to quantify the suspended load of sediment transport, while the bed shear stress is pertinent to determine the bed load of sediment transport. Kuhnle et al. [14] examined the three-dimensional flow field around a submerged spur dike. An amplification factor of bed shear stress 3 was found. Duan et al. [7] measured the flow and turbulence around an experimental spur dike in a flat and scour bed. Differences of mean velocity, turbulent intensity, and Reynolds stresses between those two flow fields were analyzed. The bed shear stress calculated from the Reynolds stresses was 2-3 times that of the incoming flow. Since the abutment and spur dike have similar contraction impact on the flow, all the three studies showed similar amplification factor of bed shear stress in open channel flow.

## 1.2. Impact of ice cover

Extensive studies have been conducted to study the local scour around structures in the past few decades. However, most of the previous studies were focused on flow in open channels. The impact of ice cover on local scour has not been well understood. For many regions in the northern hemisphere, winter may last up to six months. Figure 1 shows the ice cover around Ambassador Bridge, Windsor, Canada, which is located on the Detroit River. It can be seen from Figure 1 that the region around the pier is completely covered by ice. The presence of the ice cover affects the flow characteristics of the river. Hence, further research on the impact of ice cover on the local scour around bridge piers becomes important.

As pointed out by Morse and Hicks [21], fundamental problems of ice engineering are primarily related to ice jams, floods, and transportation over ice. River ice hydrology has been an implicit part in ice engineering. Some studies on ice engineering research can be found in the references [1,12,22,9,21,23,26,30,32]. To date, the mechanism of local scour around bridge abutments and piers under ice cover is still not well understood.

Lau and Krishnappan [15] used the  $k-\epsilon$  turbulence model to numerically determine the velocity distribution and suspended load transport under ice cover. The assumption was that the ice covered flow can be treated as two-layer flow which is divided at the location of maximum velocity. Based on the assumption that the mechanics of bed-form formation is the same for open and ice covered channels, Smith and Ettema [27] developed a method from flume data for estimating the flow resistance in ice covered channels. Ettema et al. [8] proposed a different approach to estimate the sediment transport under ice cover by using the procedures from open channel flow. The variation of ice cover roughness and flow cross sections under ice cover can limit the accuracy of this method. Ettema and Daly [9] conducted a series of flume experiments on the sediment transport under ice cover. Since the flow distribution is substantially modified by ice cover, the sediment transport under ice cover is hard to estimate. Sui et al. [26] conducted a series of flume experiments for the incipient motion under different flow

and boundary conditions. The influence of ice cover roughness has been assessed. They found that the slope of ice cover has a great impact on the critical dimensionless shear stress for the river sediment motion.



**Figure 1.** The ice cover around bridge piers (Ambassador Bridge, Windsor, ON, Canada, 2015)

### 1.3. Impact of nonuniformity of sediment

Incipient motion of the particles is an important criterion that determines the motion of the sediment particles. When the flow attains or exceeds the criteria for incipient motion, sediment particles along the alluvial channel start to move. As defined by Yang [33], if the motion is rolling, sliding, or jumping along the bed, it is called bed load transport. If the particle is supported by the upward components of turbulent currents and stays in suspension, it is called suspended load transport.

For nonuniform sediment, no single critical grain diameter can be determined to distinguish which size of sediment moves and which does not for any specific conditions. Therefore, the incipient motion of bed material is also the beginning of armor process of the bed surface [5]. With the development of an armor layer, further sediment transport is inhibited. Since nonuniform sediment makes up the typical bed composition in natural rivers, the study of the impact of nonuniformity has to be considered with the formation of armor layer.

The forces acting on a sediment particle at the bottom of the scour hole under ice cover are shown in Figure 2. In natural rivers, the velocity profile is similar to the one shown in Figure 2, which exaggerates the impact of ice cover. Herein, the figure is used to show the impact of ice cover on velocity profile around bridge piers and abutments.

For most natural rivers, the river slopes are small enough that the component of gravitational force acting on the particle in the direction of flow can be neglected. As shown in Figure 2, the forces to be considered related to the incipient motion are the drag force  $F_D$ , lift force  $F_L$ , submerged weight  $W$ , and the resistance force  $F_R$ . The angle of the scour hole with vertical abutment is  $\alpha$ .

A sediment particle is at a state of incipient motion when the following conditions have been satisfied:

$$\begin{cases} F_D = F_R \sin \alpha \\ W = F_L + F_R \cos \alpha \end{cases} \quad (1)$$

From existing literature it is apparent that studies on local scour around hydraulic structures under ice covered conditions with nonuniform sediments are limited. The effects of ice cover and nonuniformity have to be considered in the analysis of local scour. In this chapter, Equation (1) and Figure 2 are used as the basis for analysis of incipient motion under ice cover. The force analysis of a particle under ice cover is conducted by introducing the armor layer particle size. At the end, dimensionless shear stress is calculated by using ADV (Acoustic Doppler Velocimetry) data.

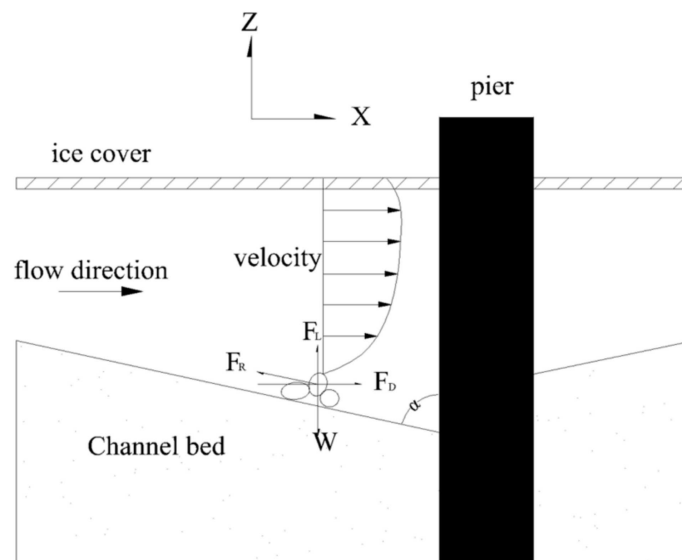


Figure 2. Incipient motion in the scour hole under ice cover (modified by [30])

## 2. Case studies

### 2.1. Experimental setup and measurement

The first case study was conducted in a 40-m long, 2-m wide, and 1.3-m deep flume with two sand boxes. The flume is a large-scale flume located at Quesnel River Research Center, BC, Canada. The aim of this case study was to investigate the ice cover impact on bridge abutment with nonuniform sediment. Smooth and rough ice covers were used. Styrofoam is commonly used to simulate ice cover in both case studies. Two different nonuniform sediments were used with  $D_{50}$  of 0.58 mm and 0.47 mm, respectively. The geometric standard deviations ( $\sigma_g$ ) were

all larger than 1.4 for the sediments, hence they can be treated as nonuniform sediment. The  $D_{90}$  of the two sediments was 2.57 mm and 1.19 mm, respectively. The sieve analysis of sediments can be found in Figure 3. Square and round abutment models were made with an equivalent diameter of 200 mm. A constant blockage of 10% was used for all experiments. Table 1 summarizes the running conditions. In all, 36 experiments were conducted.

Abutment type	Cover condition	$D_{50}$ (mm)	Water depth (m)	Approaching velocity (m/s)
Square	Open	0.58	0.07	0.26
Square	Open	0.58	0.07	0.21
Square	Open	0.58	0.19	0.21
Round	Open	0.58	0.07	0.21
Round	Open	0.58	0.19	0.23
Round	Open	0.58	0.07	0.26
Round	Smooth	0.58	0.07	0.23
Round	Smooth	0.58	0.19	0.20
Round	Smooth	0.58	0.07	0.20
Square	Smooth	0.58	0.07	0.20
Square	Smooth	0.58	0.19	0.16
Square	Smooth	0.58	0.07	0.23
Square	Rough	0.58	0.07	0.22
Square	Rough	0.58	0.07	0.20
Square	Rough	0.58	0.19	0.14
Round	Rough	0.58	0.07	0.20
Round	Rough	0.58	0.19	0.20
Round	Rough	0.58	0.07	0.22
Square	Open	0.47	0.07	0.26
Square	Open	0.47	0.07	0.21
Square	Open	0.47	0.19	0.21
Round	Open	0.47	0.07	0.21
Round	Open	0.47	0.19	0.23
Round	Open	0.47	0.07	0.26
Round	Smooth	0.47	0.07	0.23
Round	Smooth	0.47	0.19	0.20
Round	Smooth	0.47	0.07	0.20

Abutment type	Cover condition	$D_{50}$ (mm)	Water depth (m)	Approaching velocity (m/s)
Square	Smooth	0.47	0.07	0.20
Square	Smooth	0.47	0.19	0.16
Square	Smooth	0.47	0.07	0.23
Square	Rough	0.47	0.07	0.2
Square	Rough	0.47	0.07	0.20
Square	Rough	0.47	0.19	0.14
Round	Rough	0.47	0.07	0.20
Round	Rough	0.47	0.19	0.20
Round	Rough	0.47	0.07	0.22

**Table 1.** Summary of Case 1

H (mm)	Surface condition	Test Number	D (mm)	H/D	D/ $D_{50}$
108	Open channel	A1	16	6.8	31
		A2	30	3.6	59
		A3	42	2.6	82
		A4	90	1.2	176
	Ice cover	B1	16	6.8	31
		B2	30	3.6	59
		B3	42	2.6	82
		B4	90	1.2	176

**Table 2.** Summary of Case 2 (H represents flow depth; D is the pier diameter)

In each experiment, a 10 MHz SonTek ADV was used to measure the 3D flow velocity in the vicinity of abutments. For the ADV measurement, two values were used to ensure the measurements can provide an accurate representation of the flow velocity: signal-to-noise ratio (SNR) larger than 15 db and the correlation (COR) between 70% and 100%. Then, the data were analyzed by WinADV (Wahl, 2000). However, due to the limitations of ADV, the velocity profile close to the ice cover could not be measured.

The second case study was conducted at the Sedimentation and Scour Study Laboratory at the University of Windsor. The flume has a dimension of 12 m long, 1.2 m wide. The aim of this study was to investigate the ice cover impact on scour around a bridge pier. Only one type of ice cover and one uniform sediment with  $D_{50}$  of 0.51 mm was used. The sieve analysis of

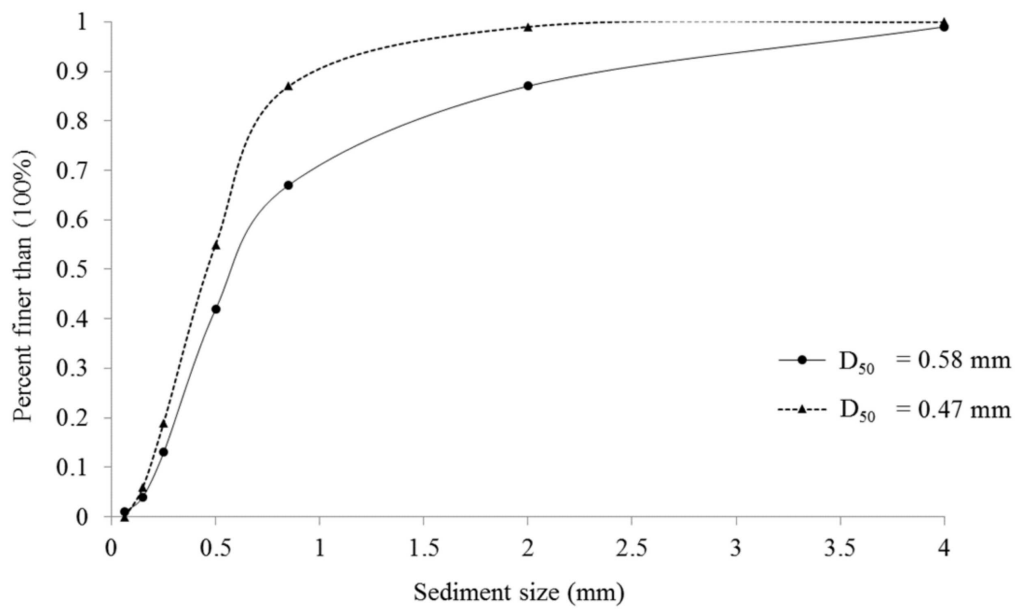


Figure 3. Sieve analysis of sediments used in Case 1

sediment is presented in Figure 4. Four pier diameters and one water depth was selected for comparison. In all, 8 experiments were conducted. Table 2 summarizes the test conditions in the case study. This study aims to investigate the ice cover impact around bridge piers with uniform sediment. A test period of 48 hours was selected to achieve near-equilibrium conditions. After each experiment, the scour profile and scour pattern were measured by using a laser point gauge.

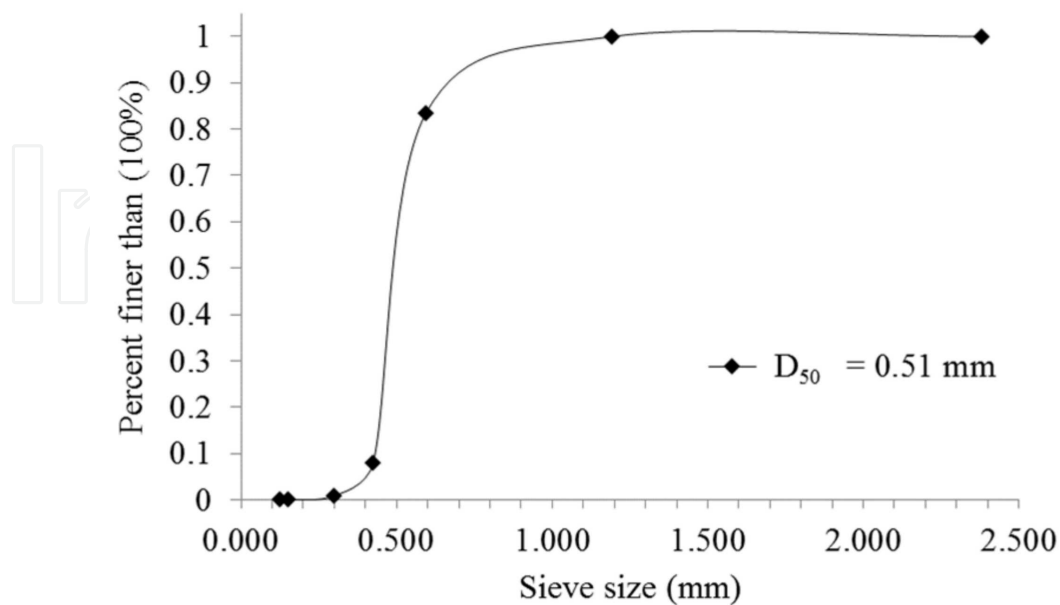


Figure 4. Sieve analysis of sediments used in Case 2

## 2.2. Results and analysis

### 2.2.1. Case 1

Figure 5 shows the scour pattern around abutments with nonuniform sediment. As shown in the figure, armor layer can be clearly noted on top of the scouring region around abutments. In both upstream and downstream of the abutment, coarse sediments were distributed equally around the scouring area. From experimental observation, the formation of armor layer greatly affects the maximum scour depth. Due to armor layer, the time needed to reach maximum scour depth is less than 24 hours.

Typical scour patterns around square and round abutments under different covered conditions were mapped. Figure 6 shows the contours around round abutment under both smooth cover and rough cover in the same flow conditions. Under both the covered conditions, the maximum scour depth is located at 60–70 degrees facing upstream. Additionally, rough cover can yield a relative larger scour compared to that from smooth cover as shown in Figure 6.

In all, 36 maximum scour depths are plotted in Figure 7, in which 18 are from a square abutment and 18 from a round abutment. Figure 7 shows the difference in maximum scour depth between the two types of abutments under different flow conditions. Based on Melville [19], the shape factor for square abutment in open channels is assumed as 1.0, while for the abutment with a round head, the value is assumed as 0.75. Figure 7 indicates that under both open channel and ice-covered conditions, square abutment generates a relatively larger maximum scour depth compared to the round abutment.

In order to compare the difference between square and round abutment, densimetric Froude number ( $F_o$ ) can be calculated by using the following:

$$F_o = U_o / \sqrt{g(\Delta\rho / \rho)D_{50}} \quad (2)$$

where  $g$  is the gravitational acceleration,  $U_o$  is the approaching velocity,  $\rho$  is the mass density of water, while the  $\Delta\rho$  is mass difference between sediment and water.  $D_{50}$  is the median grain size of sediments. An analysis using the densimetric Froude number is conducted to quantify the impact of abutment shape on maximum scour depth.

Furthermore, ice cover has a significant impact on the dimensions of the scour hole. In open channels, around the square abutment, the scour hole has a smaller slope compared to the scour holes under ice cover. It is also interesting to note that around the round abutment, the area of scour hole under the ice cover is larger than that of open channel. With the increase in ice cover roughness, there is a corresponding increase in scouring area. Around the square abutment, the scour hole retains a similar pattern with or without ice cover. While for round abutment, the scour hole under ice cover is larger than that from smooth cover and open channel.

To further examine the role of the ice cover, Figure 8 is plotted.

From Figure 8, at least two observations can be noted. Firstly, under all cover conditions, the overall trend of maximum scour depth increases with the increase in densimetric Froude number. Secondly, for a given  $F_o$ , the rough ice cover yields the largest maximum scour depth, while open channel has the smallest value. The data in Figure 8 also indicates the impact of ice cover on maximum scour depth. As mentioned previously, armor layer was detected in the scouring area around abutments.



Figure 5. Scour pattern with nonuniform sand from Case 1

Figure 9 shows armor layer sieve analysis compared with the original sediment sieve analysis. From the photos, it is interesting to note the proportion of coarse particles in the scouring area. Additionally, comparing the two analysis curves, it should become apparent that a smaller  $D_{50}$  yields small difference between armor layer and original sand, because smaller  $D_{50}$  for nonuniform sediment implies less coarse particles, hence the sediment size in the armor layer would decrease accordingly. Less coarse particles in the armor layer will provide less protection to foundation. Hence, a relatively larger maximum scour depth would be formed.

Dimensional analysis provides a convenient way for building a framework for parameters on which the maximum scour depth depends. Given the complexity of the interaction of various parameters, NCHRP [24] identified five major groups of dimensionless parameters affecting the maximum scour depth. However, there is still no clear indication on the impact of nonuniformity. In other words, the ice cover impact was not considered. Therefore, it is necessary to conduct a dimensionless analysis to investigate the ice cover impact on maximum scour depth. The following relationship can be noticed regarding maximum scour depth:

$$d_{\max} = f(U, \rho, \rho_s, g, d, n_b, n_i, D_{50}, l, B, H) \quad (3)$$

where

$d_{\max}$  is the maximum scour depth around the abutment,

$U$  is the mean approach velocity,

$\rho$  is the mass density of the water,

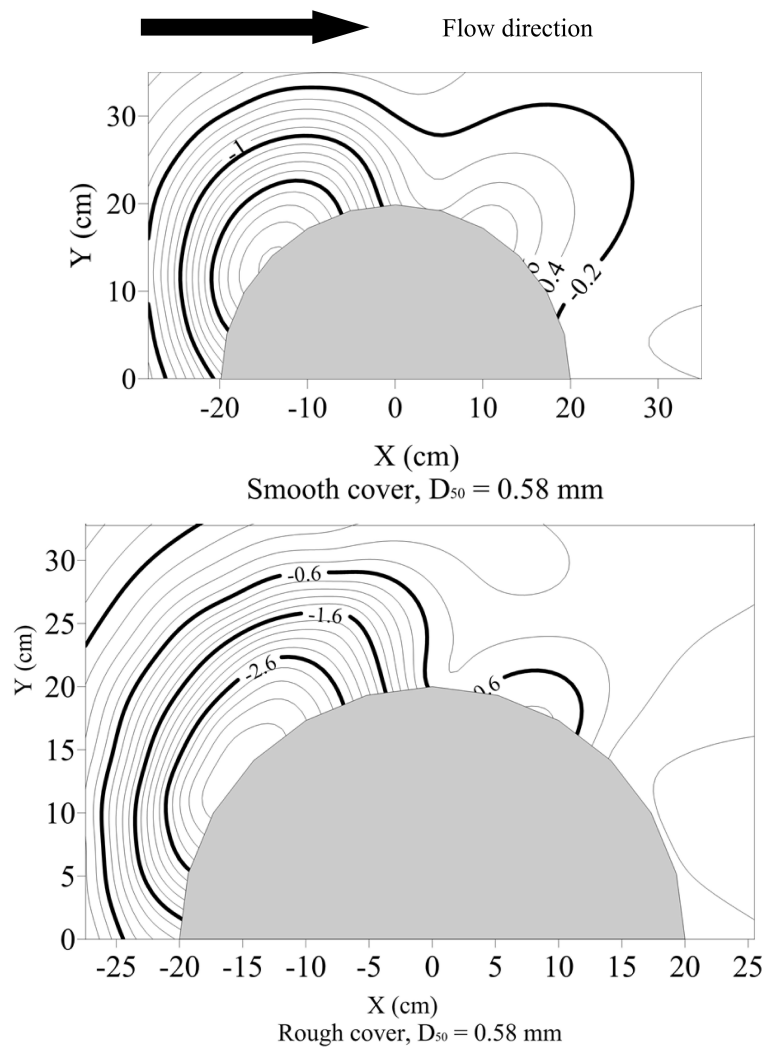


Figure 6. Scour profile around round abutment

$\rho_s$  is the mass density of nonuniform sediment,

$d$  is the armor layer grain size,

$n_b$  is the Manning's coefficient for the channel bed,

$n_i$  is the Manning's coefficient of ice cover,

$D_{50}$  is the median grain size,

$l$  is the abutment width,

$B$  is the flume width, and

$H$  is the approaching water depth.

In the above relationship, the terms  $g$ ,  $\rho$ , and  $\rho_s$  can be eliminated by introducing a combining parameter for a flow-sediment mixture. Additionally, abutment blockage ratio is also kept constant in the case study. To include the impacts of nonuniformity and armor layer, Meyer-

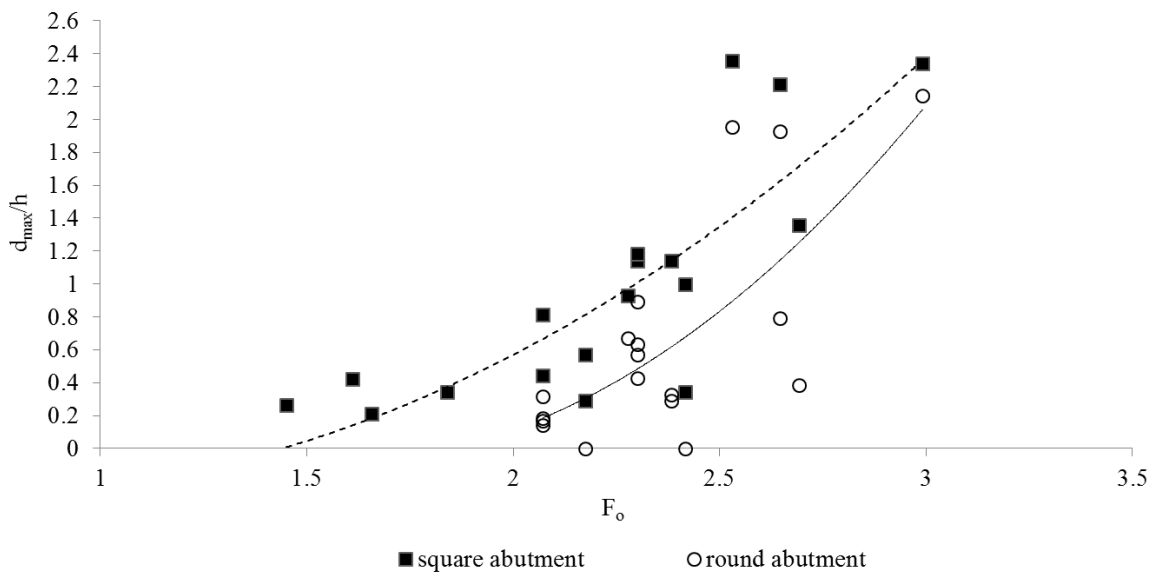


Figure 7. The dimensionless maximum scour depth variation with densimetric Froude number

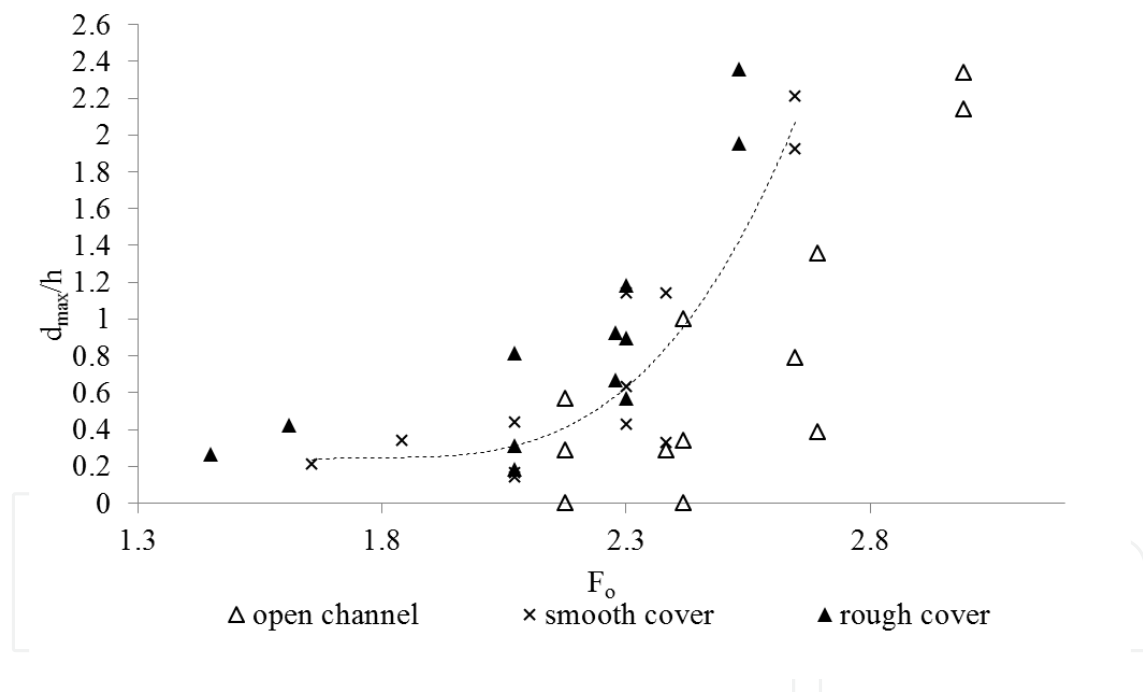


Figure 8. The comparison of dimensionless scour depth under different cover conditions (h is the flow depth)

Peter and Müller [20] developed the following equation by using one mean grain size of the bed to calculate the sediment size in the armor layer:

$$d = \frac{SD}{K_1 \left( n / D_{90}^{1/6} \right)^{3/2}} \quad (4)$$

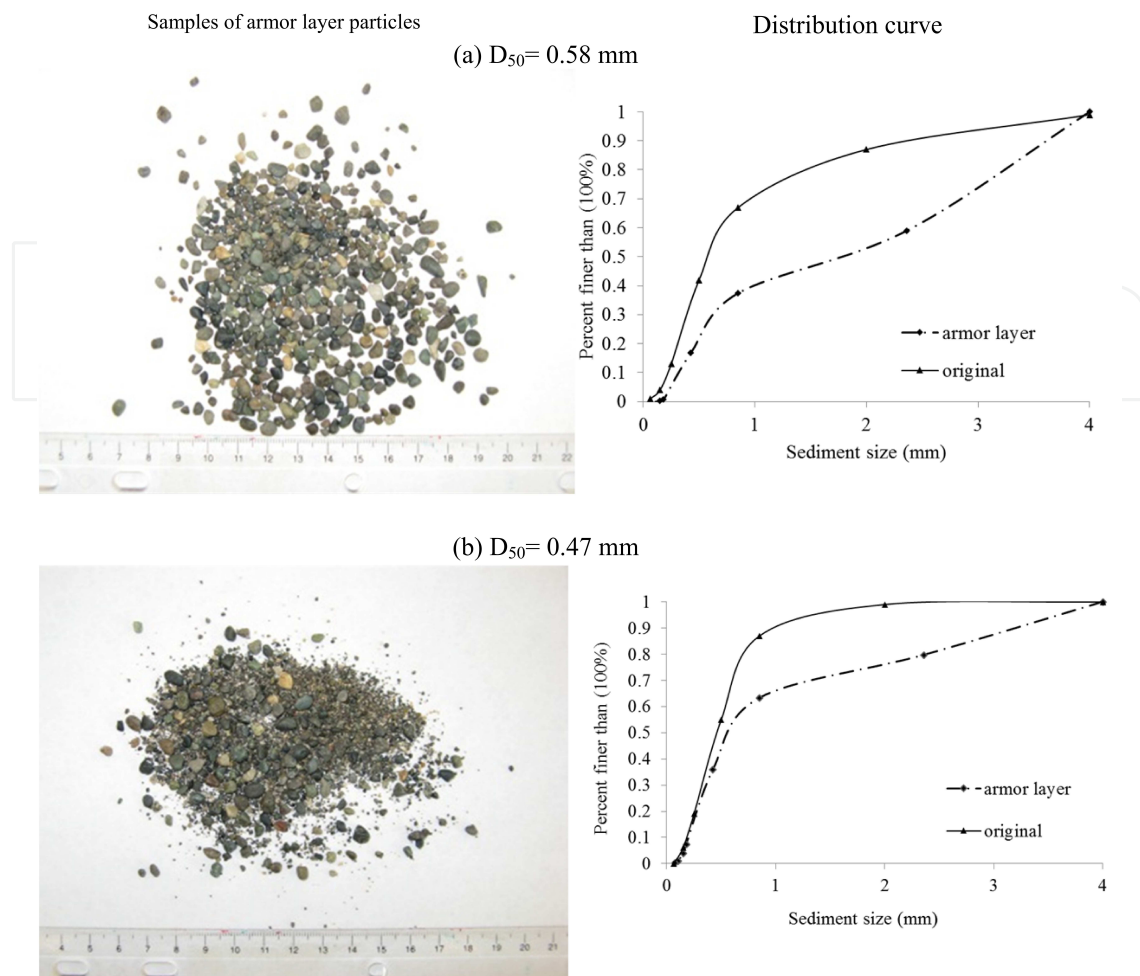


Figure 9. Samples of armor layer particle size and distribution curves

where

$d$  is the armor layer sediment size,

$S$  is the channel slope,

$D$  is the mean water depth,

$K_1$  is the constant number, which equals to 0.058 when  $D$  is in meter,

$n$  is the channel bottom Manning's roughness, and

$D_{90}$  is the bed material size where 90% of the composition is finer.

Since the armor layer particle size is of the main interest here,  $d$  is introduced in the calculation of the densimetric Froude number:

$$F_o' = U / \sqrt{(\rho_s / \rho - 1)gd} \tag{5}$$

Figure 10 shows the variation of dimensionless maximum scour depth  $d_{max}/d$  with  $F_o'$  around both square and round abutments under all three flow conditions. It should be noted that under all flow conditions, with the increase in  $F_o'$ , the value of  $d_{max}/d$  increases correspondingly. Around both square and round abutments, under the same  $F_o'$ , the rough ice cover has the largest dimensionless maximum scour depth. Smooth ice cover has the second largest value. Meanwhile, the largest dimensionless maximum scour depth is located around square abutment in all flow conditions.

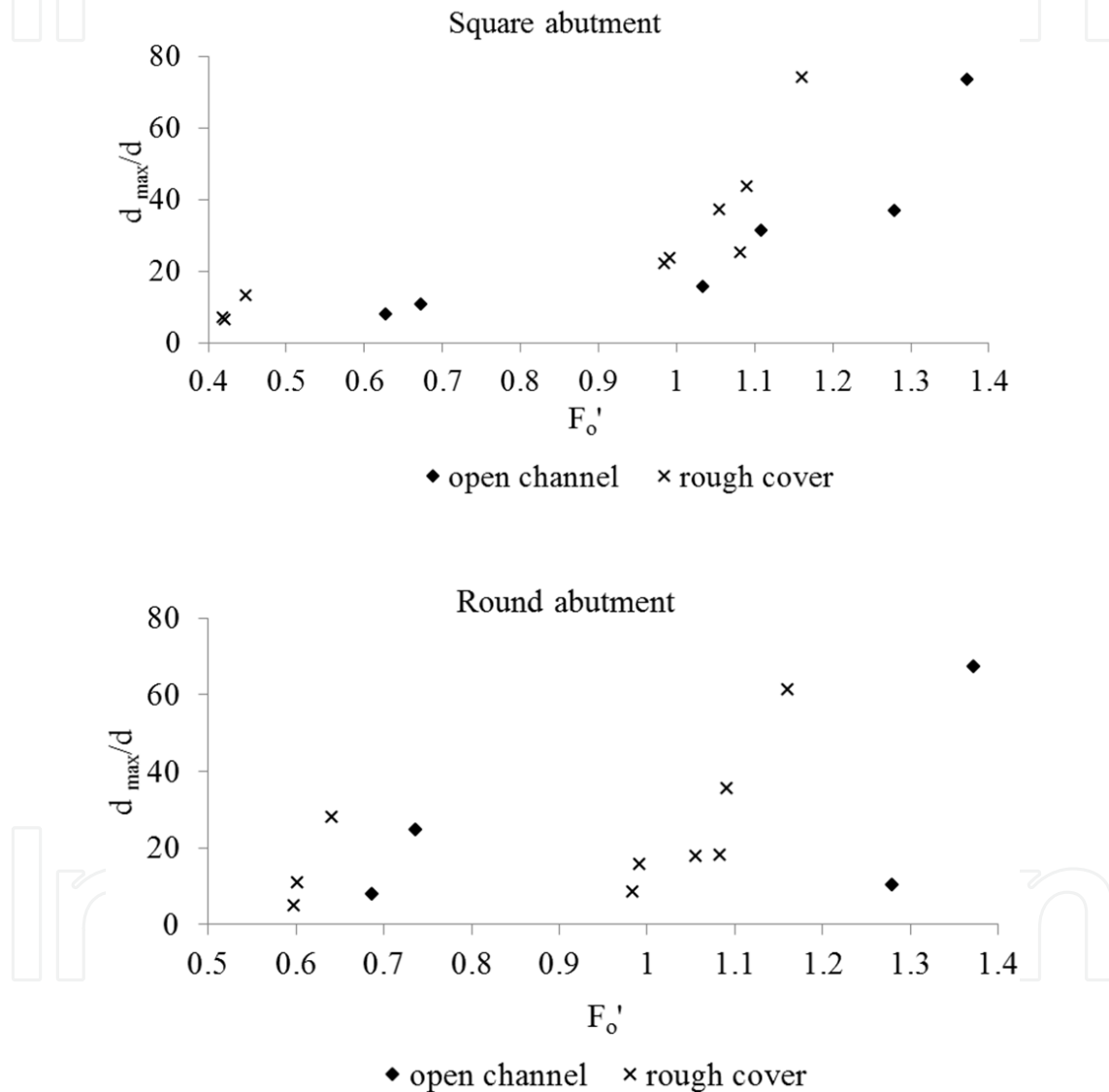


Figure 10. The dimensionless Froude number around both abutments under different cover conditions

From the above analysis, it is clear that ice cover has strong influence on local maximum scour depth around abutments. But rough ice cover has an even stronger impact.

Manning's roughness coefficient is between 0.01 and 0.0281 based on supporting field data as well as the observed ice cover characteristics [4]. In the case study, the Manning's coefficient

of 0.013 was adapted in accordance with Mays [18] for smooth ice cover. Rough ice cover was created by attaching small cubes with dimensions of 2.5 cm × 2.5 cm × 2.5 cm. The following equation was applied to calculate the Manning's coefficient [16]:

$$n_i = 0.039k_s^{1/6} \quad (6)$$

where

$k_s$  is the average roughness height of the ice underside.

In the first case study, rough ice cover has a Manning's coefficient of 0.021, which is located in the range as suggested by Carey [4]. The channel bed roughness is calculated by using the following equation from Hager [11]:

$$n_b = 0.039D_{50}^{1/6} \quad (7)$$

As suggested by Wu et al. [30], the following relationships were developed to show the maximum scour depth under ice cover around square and round abutments:

$$\left(\frac{d_{\max}}{d}\right)_{\text{square}} \sim (F_o)^{3.73} \left(\frac{D_{50}}{d}\right)^{-1.78} \left(\frac{n_i}{n_b}\right)^{0.77} \left(\frac{H}{d}\right)^{3.01} \quad (8)$$

$$\left(\frac{d_{\max}}{d}\right)_{\text{round}} \sim (F_o)^{8.60} \left(\frac{D_{50}}{d}\right)^{-4.30} \left(\frac{n_i}{n_b}\right)^{1.00} \left(\frac{H}{d}\right)^{3.00} \quad (9)$$

The exponent of each parameter from the above relationships can be used to indicate the potential impact. The exponent of  $F_o$ ,  $n_i/n_b$ ,  $H/d$  is positive, while the exponent of  $D_{50}/d$  is negative. From the previous discussion, densimetric Froude number has a positive impact on maximum scour depth. Moreover, compared to the ice cover roughness, armor layer particle size also has a strong impact on the dimensionless maximum scour depth. With the increase in armor layer particle, the maximum scour depth decreases. This conclusion is in line with a previous study conducted by Sui et al. [26]. In natural river engineering, a mixture of coarse sediments in the vicinity of bridge foundations has the potential to reduce maximum scour depth.

### 2.2.2. Case 2

Figure 11 shows the impact of ice cover on bridge pier. Only one type of ice cover was used. Some of the results are presented by Wu and Balachandar [29]. At certain water depth, in this case,  $H = 108$  mm, the scour contour and scour profile in the flow direction under ice cover is always larger than that in an open channel. The scour profiles in the flow direction also share some similarity. For example, the scour profiles almost overlap with each other in the upstream direction. While in the downstream of pier, the ice cover can clearly result in a movement of ridge toward downstream.

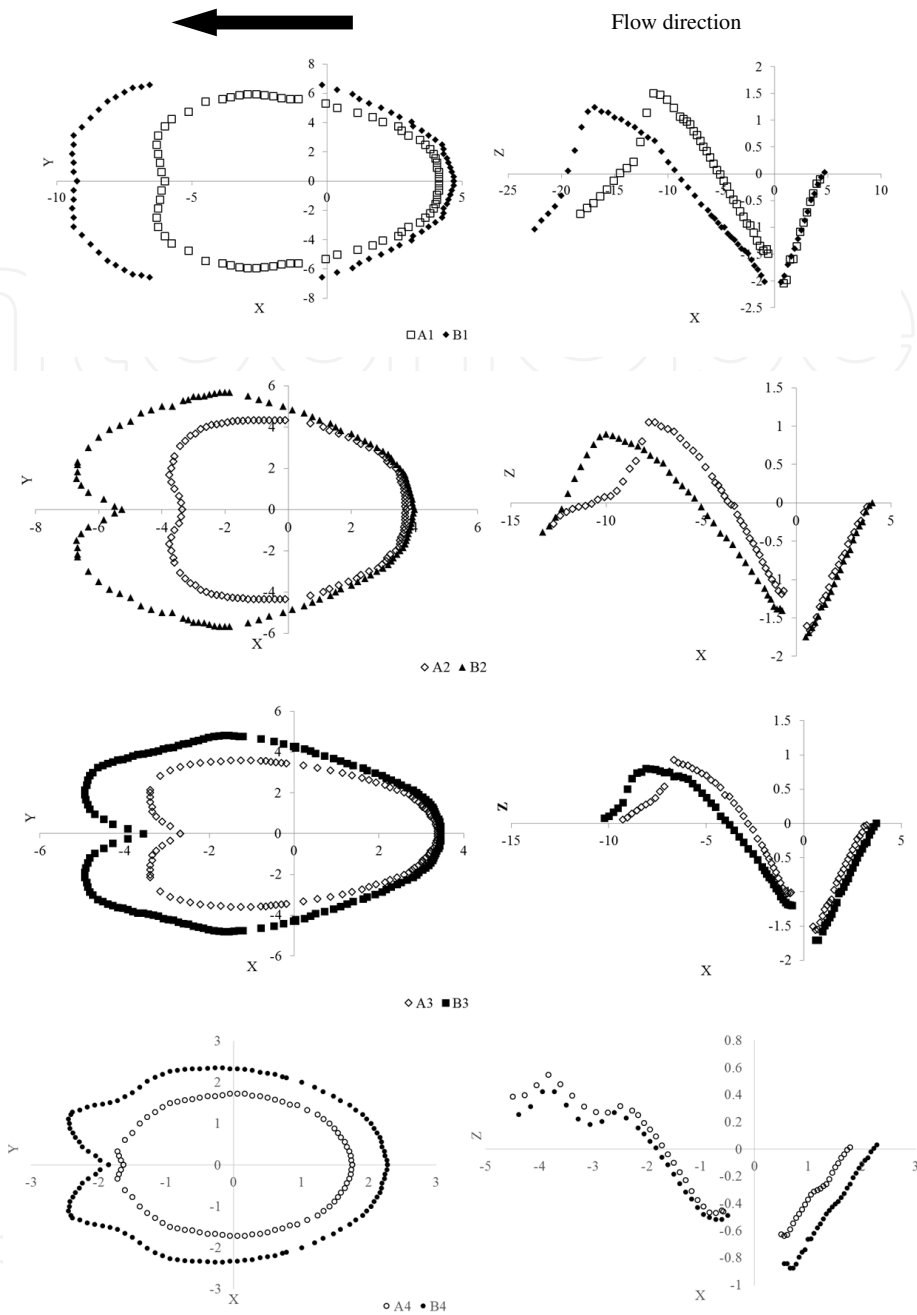


**Figure 11.** Scour comparison around piers under open channel (Group A) and ice cover (Group B) [29]

From the graphics presented above, the impact of ice cover on the local scour at bridge pier can be studied. It is evident from both case studies that, with the presence of ice cover, the maximum scour depth as well as the scour profile are increased.

### 2.2.3. Velocity profile under ice cover

By using the ADV data, the instantaneous velocity around the square abutment inside the scour hole was analyzed. The maximum scour depth is located at the upstream corner for the

square abutment. After each experiment, the velocity profile was measured at the upstream corner. Here, the parameter of interest is the maximum scour depth, so the velocity profile at the maximum scour depth location was plotted. The three-dimension velocity  $u$ ,  $v$ ,  $w$  in open channel, under both smooth ice cover, and rough ice cover are plotted in Figures 12 and 13.

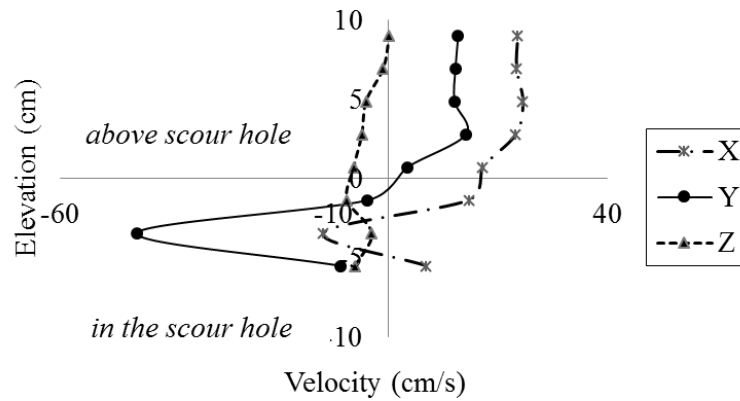
For different sediments, the velocity profiles in the scour hole are slightly different. From these figures, one can notice the following:

- In open channel, the velocity in the X direction (flow direction) has the largest magnitude, while the velocity in Y direction (transverse direction) is second largest. One can also observe in open channel, the velocity in the X and Y directions changes direction from positive to negative or from negative to positive. Compared to the change of velocity direction in X and Y directions under ice cover, the open channel has the most turbulence in both the X and Y directions.
- Under ice-covered condition, the velocity magnitude in the Y direction has the largest magnitude followed by the velocity magnitude in X direction. This trend is clear in Figure 13 under both smooth and rough ice cover. At the same flow depth, the velocity in the Y direction inside the scour hole under rough ice cover has the largest value.
- Due to the impact of ice cover on the flow, the velocity in the Z direction is significantly different compared to that of open channels. Under ice-covered condition, the magnitudes in Z direction are larger than that from open channels. While under rough ice cover, the velocity gradient in Z direction is the largest. With decreasing  $D_{50}$ , the velocity in Z direction increases correspondingly. This is attributed to the presence of ice cover, which pushes the flow down toward the channel bed. A larger scour depth is formed. With the increase in ice cover roughness, the velocity in Z direction is increased correspondingly. With the decrease in  $D_{50}$  and increase in ice cover roughness, the variation of velocity in Z direction is obvious.
- Above the scour hole, the velocity gradients in both X and Y directions are decreased. The maximum velocity in X and Y direction is located at about the mid-depth from bottom of scour hole to the ice cover as shown in Figure 13.

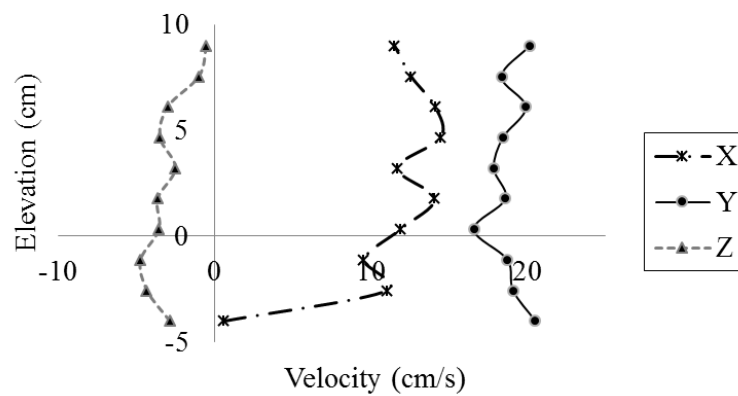
#### 2.2.4. Shear stress analysis

Bed shear stress and shear velocity are fundamental variables in river hydraulics to calculate the sediment transport, scour, and deposition. Dey and Barbhuiya [6] developed the Reynolds stresses method which is widely used by engineers. Biron et al. [3] compared several methods for bed shear stress calculation. For complex flow calculation, turbulent kinetic energy (TKE) method provided the best estimate of bed shear stress as it is not affected by local streamline variation and it takes into account the increased turbulent fluctuations. Using ADV data, Biron et al. [3], MacVirar and Roy [17], and Acharya [2] concluded that the TKE method is the most reliable to estimate the bed shear stress. Acharya [2] employed the TKE method for calculating bed shear stresses around spur dikes, yielding satisfactory results.

Open channel



Smooth cover



Rough cover

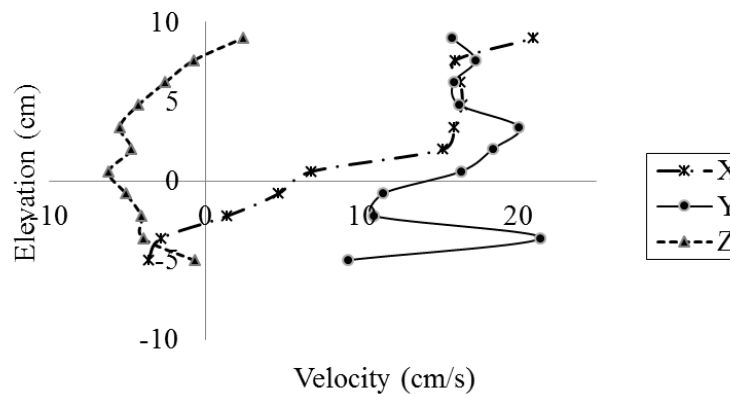


Figure 12. Three-dimensional velocity profile under different cover conditions ( $D_{50} = 0.58$  mm)

Near-bed velocities were measured by placing the ADV probe in the scour hole. Three-dimensional velocity vectors were collected. For the instantaneous velocity component  $u$ ,  $v$ ,  $w$  in the X, Y, Z direction, the time-averaged velocity can be given as:

$$u = \bar{u} + u', v = \bar{v} + v', w = \bar{w} + w' \quad (10)$$

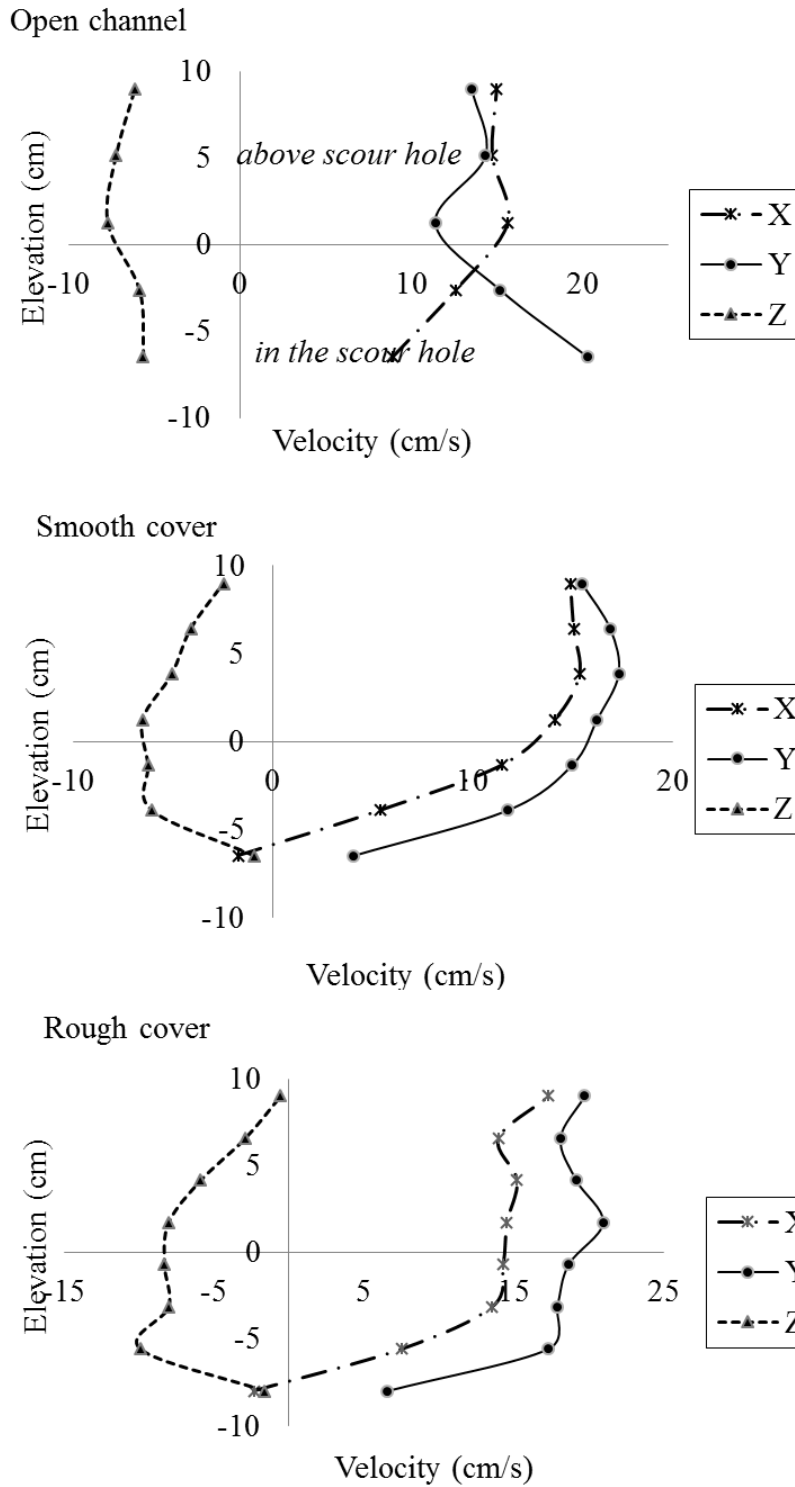


Figure 13. Three-dimensional velocity profile under different cover conditions ( $D_{50} = 0.47$  mm)

where  $u'$ ,  $v'$ ,  $w'$  denote the turbulent fluctuations in X, Y, and Z directions. The collected velocities at each point were processed to calculate the mean flow and turbulence characteristics at each point.

The bed shear stress was calculated by using TKE method as:

$$\tau_b = C_1 \left[ \frac{1}{2} \rho (u'^2 + v'^2 + w'^2) \right] \quad (11)$$

where  $C_1$  is a proportionality constant which equals 0.19 [13]. Due to the fact that instrument noise errors associated with vertical velocity fluctuations were smaller than that of the horizontal velocity fluctuations, the above equation then can be simplified as:

$$\tau_b = C_2 \rho (w'^2) \quad (12)$$

where  $C_2 = 0.9$ .

From discussions in Section 2.2.3, the velocity in Z direction plays a crucial role for the scouring process under ice cover. Hence, the above equation was used for calculation. The total bed shear stress in the scour hole can be expressed in dimensionless form as:

$$\hat{\tau} = \tau_b / \tau_0 \quad (13)$$

where  $\tau_0$  is the bed shear stress of the approaching flow calculated from  $\tau_0 = \rho U_{*c}^2$ , where  $U_{*c}$  is the critical shear velocity.

Figure 14 shows the variation of dimensionless shear stress at different elevations around the square abutment in open channel flow, smooth ice cover, and rough ice cover. The following conclusions can be drawn:

- Under rough ice cover condition, the rate of change of dimensionless shear stress is the largest compared with smooth ice cover and open channel. A larger bed shear stress is needed for the incipient motion in the scour region.
- Finer particles need relatively less dimensionless shear stress for the scouring under the same flow and cover conditions.
- Under rough ice cover condition, the dimensionless bed shear stress at the underside of ice has a relatively large magnitude. Additionally, the variation of dimensionless shear stress under ice cover has a shape of "S" as shown in Figure 14. However, more research should be conducted to validate this.

### 3. Conclusion

Ice cover and nonuniform sediment are two critical parameters for the development of scour around hydraulic structures, such as bridge piers and abutments. By using two case studies,

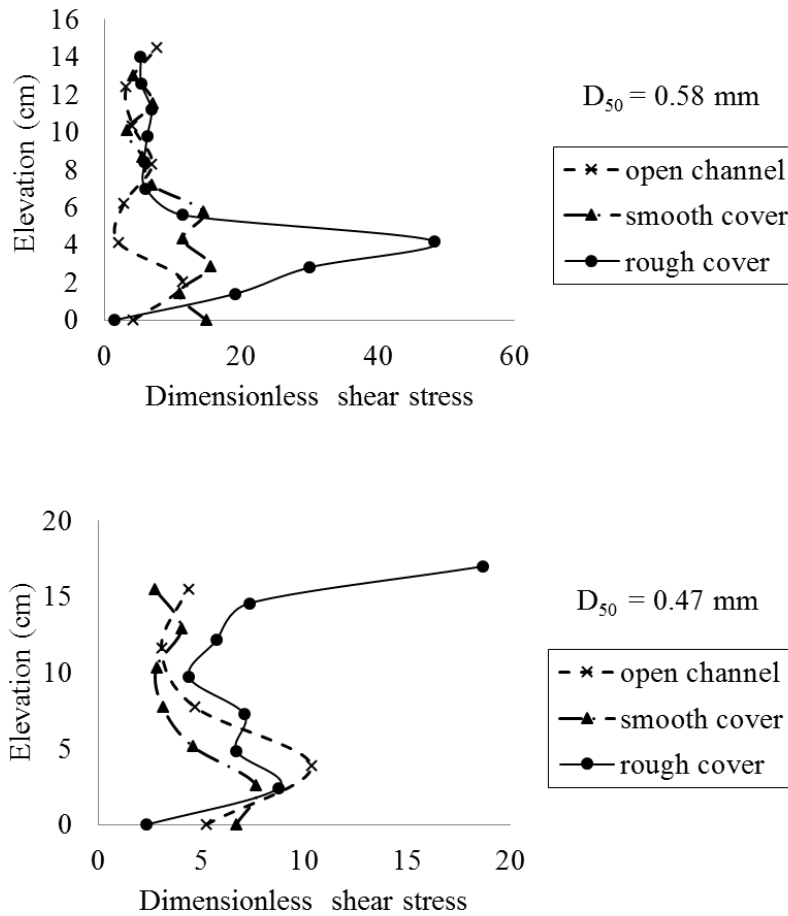


Figure 14. Comparison of measured dimensionless shear stress under different conditions

the impact of ice cover is presented in the chapter. With an increase in the densimetric Froude number, there is a corresponding increase in the dimensionless scour depth. For same nonuniform sediment, due to the formation of armor layer, less maximum scour depth was noted around bridge foundation structures. The increase in ice cover roughness can also result in a larger scour depth and profile. By analyzing the ADV data collected from Case 1, it was found that the velocity magnitude in Z direction is larger under ice covered flow in the scour hole than that under open channel flow. The velocity magnitude in Y direction has the largest magnitude under ice cover. More research is required to gain sufficient insight into the impact of ice cover on the local scour around hydraulic structures.

### Acknowledgements

Experimental work was conducted at Quesnel River Research Center (QRRRC), Likely, BC, and Sedimentation and Scour Study Laboratory at University of Windsor. Staff and colleagues provided great help.

## Author details

Peng Wu<sup>1</sup>, Jueyi Sui<sup>2</sup> and Ram Balachandar<sup>3</sup>

\*Address all correspondence to: Peng.Wu@uregina.ca

1 Environmental Systems Engineering, University of Regina, Canada

2 Environmental Engineering Program, University of Northern British Columbia, Canada

3 Civil and Environmental Engineering, University of Windsor, Canada

## References

- [1] Ackermann N L, Shen H T, Olsson P, 2002. Local scour around circular piers under ice covers. *Proceeding of the 16th IAHR International Symposium on Ice*, International Association of Hydraulic Engineering Research, Dunedin, New Zealand.
- [2] Acharya A, 2011. Experimental study and numerical simulation of flow and sediment transport around a series of spur dikes, PhD thesis, The University of Arizona, pp. 140-161.
- [3] Biron P M, Robson C, Lapointe M F, Gaskin S J, 2004, Comparing different methods of bed shear stress estimates in simple and complex flow fields. *Earth Surf Process Landforms*, Vol. 29, pp. 1403-1415.
- [4] Carey K L, 1966. Observed configuration and computed roughness of the underside of river ice, St Croix River, Wisconsin, Professional paper 550-B, US Geological Survey, pp. B192-B198.
- [5] Chien N, Wan Z, 1999. *Mechanics of Sediment Transport*. ASCE Process. Reston, Virginia, USA.
- [6] Dey S, Barbhuiya A K, 2005. Turbulent flow field in a scour hole at a semicircular abutment, *Can J Civil Engin*, Vol. 32, pp. 213-232.
- [7] Duan J G, He L, Fu X, Wang Q, 2009, Mean flow and turbulence around experimental spur dike, *Adv Water Res*, Vol. 32, pp. 1717-1725.
- [8] Ettema R, Braileanu F, Muste M, 2000. Method for estimating sediment transport in ice covered channels, *J Cold Region Engin*, ASCE, Vol. 14, No. 3, pp. 130-144.
- [9] Ettema R, Daly S, 2004. Sediment transport under ice. ERDC/CRREL TR-04-20. Cold Regions Research and Engineering Laboratory U.S. Army Engineer Research and Development Center 72 Lyme Road Hanover, New Hampshire 03755.

- [10] Goring D G, Nikora V I, 2002, Despiking acoustic Doppler velocimeter data. *J Hydraul Engin, ASCE*, Vol. 128, No. 1, pp. 117-126.
- [11] Hager W H, 1999. *Wastewater Hydraulics: Theory and Practice*, Springer, Berlin, New York, pp. 17 – 54.
- [12] Hains D B, 2004. An experimental study of ice effects on scour at bridge piers, PhD Dissertation, Lehigh University, Bethlehem, PA.
- [13] Kim S C, Friedrichs C T, Maa J P Y, Wright L D, 2000. Estimating bottom stress in tidal boundary layer from acoustic Doppler velocimeter data, *J Hydraul Engin*, Vol. 126, No. 6, pp. 399-406.
- [14] Kuhnle R A, Jia Y, Alonso C V, 2008. Measured and simulated flow near a submerged spur dike, *J Hydraul Engin, ASCE*, Vol. 134, No. 7, pp. 916-924.
- [15] Lau Y L, Krishnappan B G, 1985. Sediment transport under ice cover, *J Hydraul Engin, ASCE*, 111(6), pp. 934-950.
- [16] Li S S, 2012. Estimates of the Manning's coefficient for ice covered rivers, *Water Management, Proc Institut Civil Engin*, Vol. 165, Issue WM9, pp. 495-505.
- [17] MacVirar B J, Roy A G, 2007. Hydrodynamics of a forced riffle pool in a gravel bed river: Mean velocity and turbulence intensity, *Water Res Res*, Vol. 43, Issue 12, DOI: 10.1029/2006WR005272.
- [18] Mays L W, 1999. *Hydraulic Design Handbook*, McGraw-Hill, pp. 3.12.
- [19] Melville B W, 1997. Pier and Abutment scour: integrated approach, *J Hydraul Engin, ASCE*, Vol. 123(2), pp. 125-136.
- [20] Meyer-Peter E, Müller R, 1948. Formula for bed-load transport, Proceedings of International Association for Hydraulic Research, 2nd Meeting, Delft, Netherlands, pp. 39-64.
- [21] Morse B, Hicks F, 2005. Advances in river ice hydrology 1999-2003, *Hydrol Process*, Vol. 19, Issue 1, pp. 247-263.
- [22] Munteanu A, 2004. Scouring around a cylindrical bridge pier under partially ice-covered flow condition, Master thesis, University of Ottawa, Ottawa, Ontario, Canada.
- [23] Munteanu A, Frenette R, 2010. Scouring around a cylindrical bridge pier under ice covered flow condition-experimental analysis, R V Anderson Associates Limited and Oxand report.
- [24] NCHRP Web-only Document 181, 2011. Evaluation of Bridge-Scour Research: Abutment and Contraction Scour Processes and Prediction. NCHRP Project 24-27(02).
- [25] Rehmel M, 2007. Application of Acoustic Doppler Velocimeter for streamflow measurements, *J Hydraul Engin, ASCE*, Vol. 133, Special Issue: Acoustic Velocimetry for Riverine Environments, pp. 1433-1438.

- [26] Sui J, Wang J, He Y, Krol F, 2010. Velocity profile and incipient motion of frazil particles under ice cover, *Int J Sedim Res*, Vol. 25(1), pp. 39-51.
- [27] Smith B T, Ettema R, 1997. Flow resistance in ice covered alluvial channels, *J Hydraul Engin ASCE*, Vol. 123(7), pp. 592-599.
- [28] Wahl T L, 2000, Analyzing data using WinADV, 2000 Joint Conference on water resources engineering and water resources planning and management, Minneapolis, Minnesota, pp. 1-10.
- [29] Wu P, Balachandar R, 2015. Measurement of scour profiles around bridge piers in channel flow with and without ice-cover, 22nd Canadian Hydrotechnical Conference, April 29-May 3, Montreal, Quebec, Canada, pp. 1-11.
- [30] Wu P, Hirshfield F, Sui J, 2014a, Armor layer analysis of local scour around bridge abutments under ice cover. *River Research and Applications*, published online in Wiley Online Library, DOI: 10.1002/rra.2771.
- [31] Wu P, Hirshfield F, Sui J. 2014b, Further studies of incipient motion and shear stress on local scour around bridge abutment under ice cover, *Can J Civil Engin*. Vol. 41(10), pp. 892-899.
- [32] Wu P, Hirshfield F, Sui J, 2015. Local scour around bridge abutments under ice covered conditions – an experimental study, *Int J Sedim Res*, Vol. 30 (1), pp. 39-47.
- [33] Yang C T, 2003. *Sediment Transport, Theory and Practice*. Krieger Publishing Company, Krieger Drive, Malabar, Florida 32950.

